Longitudinal and Transversal End Effects Analysis of Linear Switched Reluctance Motor

Zhu Zhang, Norbert C. Cheung, Senior Member, *IEEE*, K. W. E. Cheng, Senior Member, *IEEE*, X. D. Xue， Member, *IEEE*, and J. K. Lin

Department of Electrical Engineering, The Hong Kong Polytechnic University, Hung Hom, Kowloon, Hong Kong

An accurate estimation of flux linkage characteristics is very important during the preliminary design stage and high-performance control of linear switched reluctance motor (LSRM). In this paper, longitudinal and transversal end effects of a double-side LSRM are studied using analytical method and finite element analysis (FEA). The estimation discrepancy introduced by both end effects is presented respectively by investigating their sensitivities to machine parameters, such as excitation level, translator position and stack length.

***Index Terms*—End Effect, Energy Conversion Principle, Finite Element Analysis, LSRM**

I. Introduction

Linear switched reluctance motors (LSRMs) have simple and robust structure, and become attractive candidate for high performance motion system [1]. Like other linear motors, there is extra longitudinal end effect in LSRMs, due to the finite length of the stator stack. It is important to predict the accurate relationships between the flux linkages and excitation currents at different translator positions during the design stage. The data is required to calculate the work done at one stroke and then the electromagnetic force. However, inherently nonlinear behavior introduced by doubly salient structure and deep saturation makes it difficult to obtain the performance characteristic curves.

Several analytical methods, which are based on motor geometry and core magnetization curve, were proposed to compute the flux linkages. It is possible to generate accurate results for aligned position due to the omission of leakage flux, but it may bring large discrepancy in calculating the flux linkages for unaligned positions. Hence, analytical method is more suitable for qualitative understanding of the effects of dimensional changes and preliminary machine design.

Two-dimensional finite element analysis (2D FEA) is widely used in predicting the performance characteristics for its simplicity and fast calculation time. Satisfactory results can be ensured for LSRMs with long stack length or low saturation. The prediction accuracy becomes insufficient as the stack length gets shorter, because the transversal end effect, which is ignored in 2D FEA, becomes more dominant in short stack machine. The most accurate prediction results can be obtained by the three-dimensional finite element analysis (3D FEA). Transversal end effect is included, but this approach will significantly increase the computation time, especially in calculating the flux linkages of LSRMs [2]. Quite a lot of solutions would be required at a wide range of excitation currents and translator positions.

Since the longitudinal and transversal end effects would induce errors in estimating the performance characteristics of LSRMs, it is necessary to study their sensitivities to machine parameters, such as geometric topology, stack length, excitation level and translator position.

II. Problem Description

1) Linear Switched Reluctance Motor

A four-phase double-side linear switched reluctance motor was constructed to study the impact of end effects, as shown in Fig. 1. The detailed specification is listed in Table I. It can be observed that the iron stack length is quite short according to the length of stator pitch. Hence, the end effects have to be considered if more accurate prediction is required. The 2D FEA model is based on the YZ plane cross section. By adjusting the excitation current and shifting the translator poles, we can obtain the flux linkage curves and static force profiles for one stroke operation.

FIG. 1 & TABLE 1 HERE

2) Energy Conversion Principle

The steady-state and dynamic-state performance of LSRM can be evaluated by calculating the energy conversion for one stroke. Consider the energy conversion procedure of one phase as shown in Fig. 2. Assuming translator moves for a distance dx under the action of force F, the mechanical work is thus

$$dW_m = Fdx \tag{1}$$

If losses are neglected, the amount of electrical energy W_e is transferred into the magnetic field W_f and mechanical work dW_m, which can be written as in (2)

$$dW_e = dW_f + dW_m \tag{2}$$

From the above equations, we can write down

$$dW_f = dW_e - Fdx = id\lambda - Fdx \tag{3}$$

If we define the area between the aligned and unaligned curves as the coenergy W_f', which does not exist physically, we can obtain

$$dW_f'(i,x) = \lambda di + Fdx = \frac{\partial W_f'(i,x)}{\partial i}di + \frac{\partial W_f'(i,x)}{\partial x}dx \tag{4}$$

Therefore,

$$\lambda = \frac{\partial W_f'(i,x)}{\partial i} \tag{5}$$

$$F = \frac{\partial W_f'(i,x)}{\partial x} \tag{6}$$

From the diagram shown in Fig. 2, the coenergy that between two magnetization curves can be calculated by

$$W_f'(i,x) = \int_0^i (\lambda_{x+dx}(i,x) - \lambda_x(i,x))di \quad (7)$$

FIG. 2 HERE

The solid flux linkage curves are calculated by assuming end-effects, and other two curves in dashed lines are calculated by neglecting two end-effects. It can be observed that the omission may reduce the energy conversion area and lowers the performance calculation.

III. Longitudinal End Effect

A fundamental difference between a rotary switched reluctance motor (RSRM) and an LSRM is the finite length of the magnetic and electric circuit of the LSRM in the direction of the travelling field [3]. The finite length of stator stack causes an unbalanced phase inductance, which is the so-called longitudinal end effect in LSRM. The performance characteristics of phase A at the end and phase B in the middle are illustrated in Fig. 3. There is certain discrepancy between these two phases. This effect must be carefully considered in evaluating the flux linkage per phase in high performance motion control.

FIG. 3 & FIG. 4 HERE

The equivalent circuit approach is very useful for analyzing the cause of the longitudinal end effect. The disparity can be easily derived from the steady-state equivalent circuit. To simplify the analysis, transversal end effect is neglected here. Thus 2D FEA is adequate to verify the analysis and determine the sensitivities to machine parameters.

The distribution of the magnetic flux lines of two phases in unaligned position are shown in Fig. 4. It is observed that the leakage flux lines of phase B pass through the stator slot to both adjacent stator poles and enclose the path through the stator back iron, while the end phase A has only one adjacent stator pole and the leakage flux lines at this side have to be enclosed with air. As we know, the longer is the leakage flux path in stator, the higher is the phase inductance. Therefore, the inductance of phase A is smaller than that of phase B. The same situation goes in aligned position and in-between positions.

In order to illustrate the sensitivities to machine parameters, 2D FEA is used to study the longitudinal end effect. The inductance variation with excitation and translator position of per phase were calculated and compared.

A. Inductance variation with excitation current

As we can see from Fig. 5, the error percentage of inductance between phase A and phase B is basically constant in unaligned position. It can be observed that the inductance of phase A, over the excitation range, can be decreased by up to 13%, owing to the longitudinal end effect. The error percentage of inductance in aligned position is slightly decreased as the excitation current increased. Owing to the large airgap in unaligned position, the error in aligned position remains small over the excitation range.

FIG. 5 & FIG. 6 HERE

B. Inductance variation with translator position

The variation of error percentage with translator position under rated excitation is illustrated in Fig. 6. Zero in position axial represents the fully unaligned position. It can be seen that the error percentage reached a peak value near the unaligned position, and then gradually decreased as the translator pole moves into alignment with the excited stator pole. This is due to the fact that the leakage flux decreases as the pole overlap increases when the poles are not saturated.

C. Solutions

The longitudinal end effect causes an unbalanced phase characteristics and brings a certain discrepancy in predict the actuator performance. The easiest way to compensate the decrease of inductance of the end phase is to add an extra pair of stator poles at both ends of the stator. However, this solution may increase the length of stator and is not suitable for the application that has limited space.

IV. Transversal End Effect

2D FEA is widely used to verify the design and predict the performance characteristics for its simplicity and fast computation. However, all practical machines are three-dimensional, therefore two-dimensional model based analysis will be inadequate in many cases due to the omission of transversal end effects. It can be observed from Fig. 7 that the values of flux linkage are underestimated by 2D FEA and hence a reduced energy conversion area is obtained. Therefore, it is necessary to identify the relationships between 2D and 3D FEA results and determine the sensitivity of transversal end effects to motor parameters.

FIG. 7 HERE

There are three different causes that contribute to the end effects: axial fringing, end-winding flux and anisotropy of lamination [4]. Axial fringing exists at both ends of the machine stack, and magnetic flux tends to bulge out axially from the stator pole ends into the translator pole ends. The inductance in unaligned position is considered to be increased by 20-30% owing to the fringing effect [5]. As the phase coil is shaped like a race ring, there is conductor region that extends beyond both stack ends. The end winding inductance may account for a significant percentage of the phase inductance, especially for machine of short stack length, or long-pitched windings.

Besides the flux flowing in the plane of the laminations, there is flux flow normal to the laminations which bring significant eddy current loss. Its effective permeability is thought to be much less than that of flux in the plane laminations. Therefore, the anisotropy and directional permeability have to be considered in finite element analysis. The three-dimensional solution can be corrected by specifying a packing factor, while the two-dimensional analysis requires

a more complex method by scaling the original B-H curve according to the packing factor.

In order to identify the transversal end effect and analyze its sensitivity to actuator parameters, three-dimensional FEA was carried out and compared with the results from two-dimensional FEA solutions. The transversal end effect is proved to highly depend on the translator position, excitation level and other actuator parameters.

A. *Flux Linkage*

The variation of error percentage in flux linkage at aligned and unaligned positions with excitation current is demonstrated in Fig. 8. In the unaligned position, the error between 2D and 3D FEA is almost constant at 20% during low excitation, and begins to decrease in saturation region. This is because, at low excitation, the reluctance of airgap at unaligned position accounts for most of the magnetic circuit reluctance. While in the aligned position, the error percentage is gradually decreased as the excitation increases. This is due to the fact that the permeability of iron core is high at low excitation, and hence the end winding has greater impact on the flux linkage of phase winding.

FIG. 8 & FIG. 9 HERE

Fig. 9 illustrates the variation of error percentage with translator position due to the transversal end effect. The error percentage of flux linkage is maximal at more than 25% in unaligned position, then decreases as the overlap of the poles increases, and reaches the lowest value in the fully aligned position. This is because the saturation is getting severe as translator pole moves into alignment, and the permeability of magnetic core is reduced gradually. Therefore the end winding flux is becoming less.

B. *Stack Length*

The error incurred in 2D FEA is considered to be highly dependent on the stack length owing to the transversal end effect. Fig. 10 illustrates the variation of error percentage in flux linkage as the stack length increases. It can be observed that significant error incurred at unaligned position when the stack length is very short and the accuracy is improved obviously as the stack length is getting longer. This is due to the fact that the end winding is dominant in the phase winding conductor when the stack length is short. The error percentage at aligned position is slightly deceased and maintains at a relatively low rate.

FIG. 10 & FIG. 11 HERE

C. *Translator Stack Length*

In some application cases, the stack length of the translator is longer than that of the stator, resulting in a variation in distribution of transversal flux. The unequal axial length is hard to be reflected in 2D FEA solutions and incurs a certain error in performance prediction. The trend of impact can be examined by modeling the transversal cross section to obtain the variation of end winding inductance. As shown in Fig. 11, the inductance is gradually increased as the translator stack extents beyond the stator stack. This is because the end winding flux links more with the translator and the variation of end fringing distribution. Therefore, the error in flux linkage owing to the unequal stack length is increased as the translator stack length is getting longer.

FIG. 11 & FIG. 12 HERE

D. *Static Force*

It can be observed from Fig. 12 that at high excitations and towards alignment a higher value of static torque was predicted by 2D model solutions. This is due to the fact that in positions close to alignment the radial component of flux produced by end windings may be more dominant than tangential component [4].

V. Conclusion

The impact of longitudinal end effect in LSRM is investigated in this paper. A simple but practical solution is presented to compensate the phase imbalance introduced by the longitudinal end effect. Sensitivity analysis to machine parameters of both end effects is carried out by using 2D FEA and 3D FEA. The results obtained from FEA present the variation of estimation error with excitation current at different translator position. By understanding the impact of both end effects, the preliminary design will be more accurate and less time-consuming, and the operation performance of LSRM can be further improved.

Acknowledgment

The authors grateful acknowledge the financial support of Innovation and Technology Fund of Hong Kong SAR under the project ITP/025/09AP.

References

[1] Shi Wei Zhao, N. C. Cheung, Wai-Chuen Gan, Jin Ming Yang and Jian Fei Pan, "A Self-Tuning Regulator for the High-Precision Position Control of a Linear Switched Reluctance Motor," *Industrial Electronics, IEEE Transactions on*, vol. 54, pp. 2425-2434, 2007..

[2] Uday Deshpande, "Two-dimensional finite element analysis of a high-force-density linear switched reluctance machine including three-dimensional effects," *Industrial application, IEEE Transactions on*, vol. 36, pp. 1047-1052, 2000.

[3] J. F. Gieras, G. E. Dawson and A. R. Eastham, "A new longitudinal end effect factor for linear induction motors," *Energy conversion, IEEE Transactions on*, vol. EC-2, pp. 152-159, March 1987

[4] A. M. Michaelides and C. Pollock, "Effect of end core flux on the performance of the switched reluctance motor," *Proc. Inst. Elect. Eng.*, vol. 141, pp. 421-427, Nov. 1994

[5] A. Matveev, V. Kuzmichev and E. Lonmonva, "A new comprehensive approach to estimation of end-effects in switched reluctance motors," *Proceedings ICEM 2002*, Bruges, Belgium, August 2002.

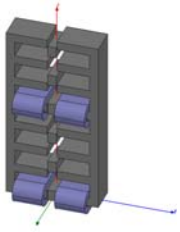

Fig. 1. Double-side LSRM

TABLE I
SPECIFICATION OF THE LSRM

Parameters	Value (mm)
stator pole width	13
stator slot width	23
translator pole width	17
translator slot width	31
stator pole height	49
translator pole height	13
stack length	43
yoke thickness	13
air gap	0.8

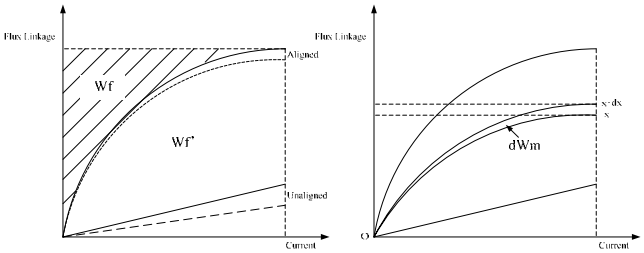

Fig. 2. Energy conversion procedure

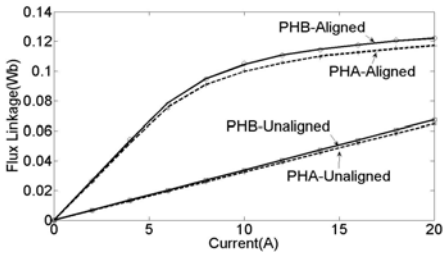

Fig. 3. Flux linkage comparison of phase A and phase B

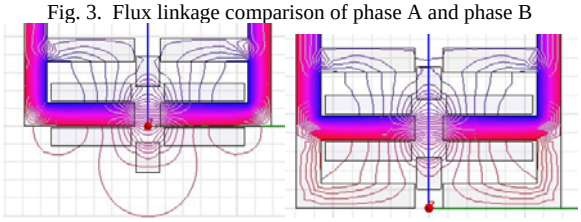

Fig. 4. Magnetic flux distribution of Phase A (left) and Phase B (right)

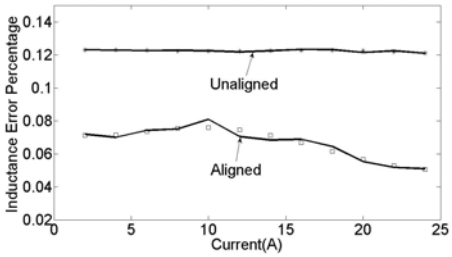

Fig. 5. Percentage variation of Inductance error with excitation current

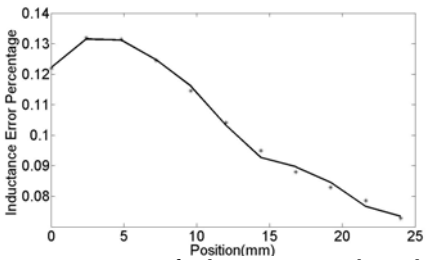

Fig. 6. Percentage variation of inductance error with translator position

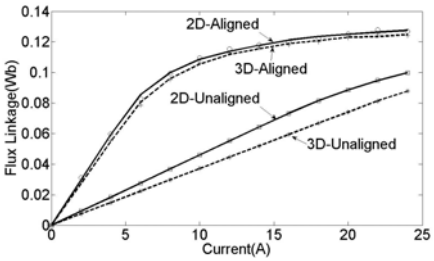

Fig. 7. Flux linkage comparison of 2D and 3D FEA

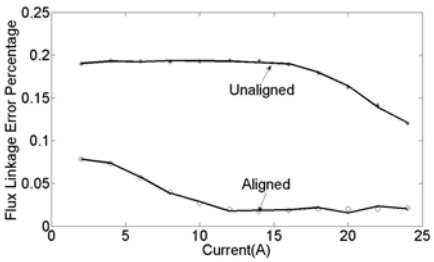

Fig. 8. Percentage variation of flux linkage error with excitation current

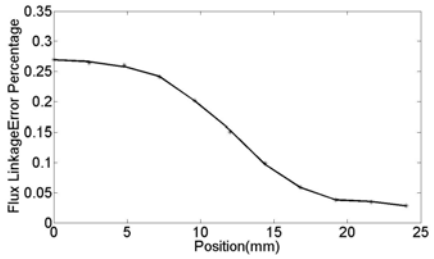

Fig. 9. Percentage variation of flux linkage error with translator position

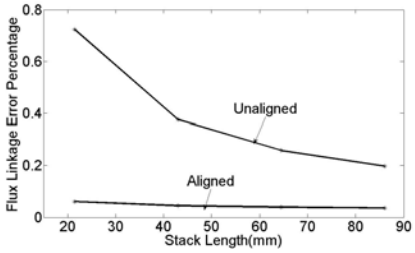

Fig. 10. Percentage variation of flux linkage error with stack length

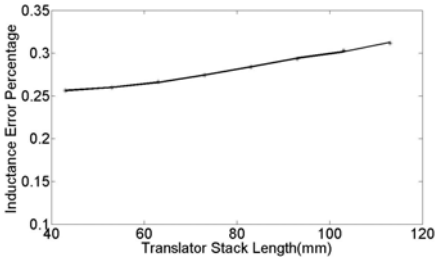

Fig. 11. Percentage variation of inductance error with translator stack length

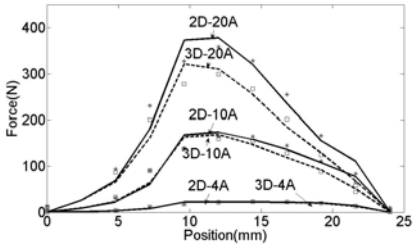

Fig. 12. Static force comparison of 2D and 3D FEA